Extreme sensitivity of graphene photoconductivity to environmental gases

Callum J. Docherty,[1] Cheng-Te Lin,[2] Hannah J. Joyce,[1] Robin J.
Nicholas,[1] Laura M. Herz,[1] Lain-Jong Li,[2] and Michael B. Johnston[1, *]

[1] *Clarendon Laboratory, Department of Physics, University of Oxford, Oxford, OX1 3PU, UK*
[2] *Institute of Atomic and Molecular Sciences, Academia Sinica, Taipei, 10617, Taiwan*

Supplementary Information

Supplementary Figures

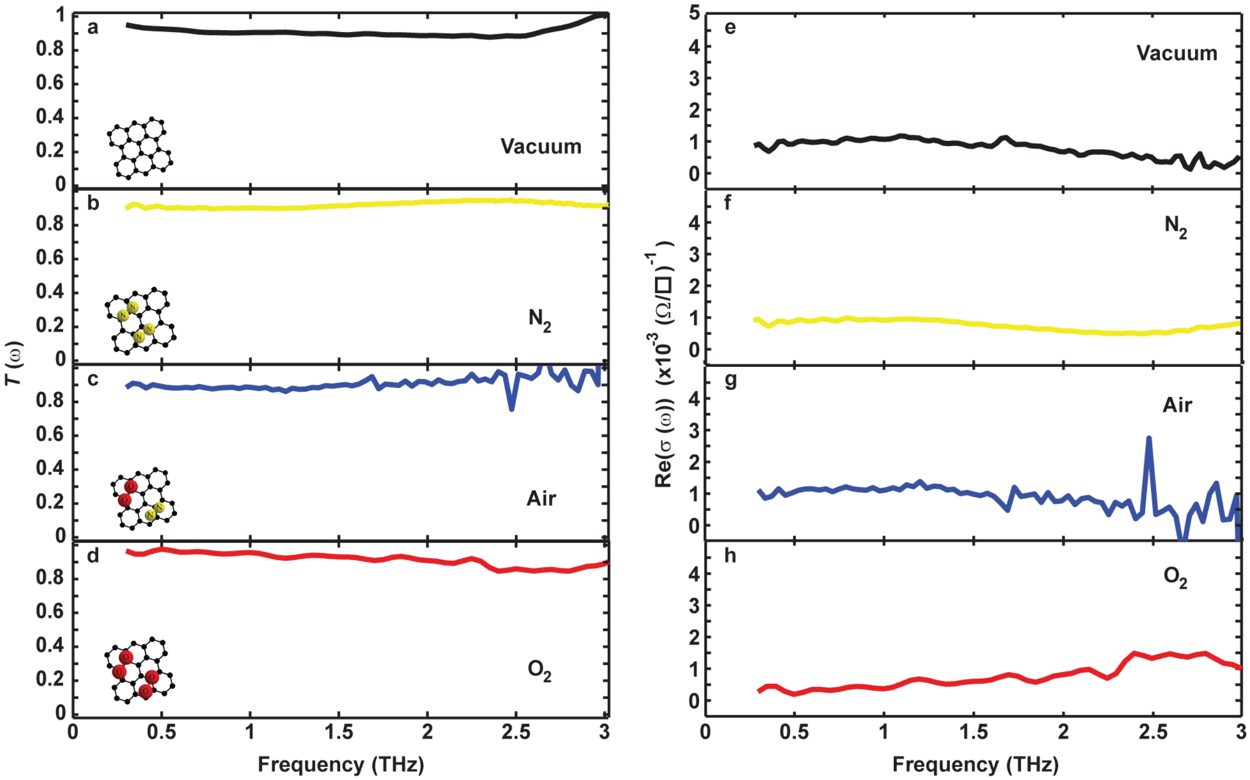

Supplementary Figure S1. Measured non–photoexcited terahertz transmission of graphene sheet in different environments. **a** In vacuum, **b** in N_2, **c** in air, **d** in O_2. **e-h** The corresponding real part of terahertz conductivity. Both transmission and conductivity are mainly constant, with no significant difference between the atmosphere types. The absorption lines in the air measurement are due to absorption of terahertz by water vapour[43].

---

[*] Electronic address: `m.johnston1@physics.ox.ac.uk`

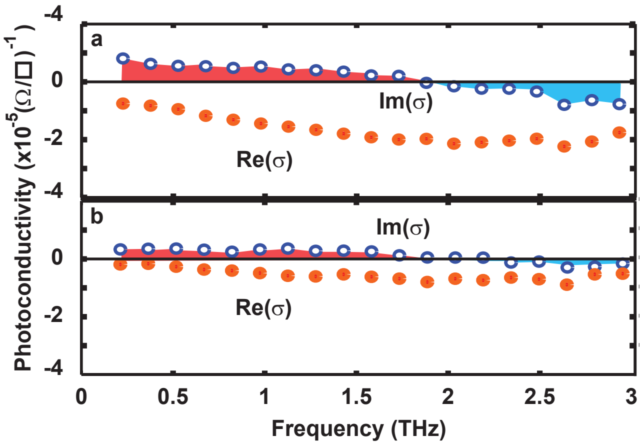

Supplementary Figure S2. Pump fluence dependence of photoconductivity spectra in air. a Photoconductivity at 2 ps after photoexcitation by 180 μJ/cm^2 pump fluence. **b** Photoconductivity at 2 ps after photoexcitation by 18 μJ/cm^2 pump fluence. Solid orange dots show the real part of the photoconductivity, hollow blue dots show the imaginary part. Shading is used to highlight the change from positive to negative Im($\Delta\sigma$), corresponding to the Lorentzian peak frequency, ω_0. ω_0 does not change with fluence, suggesting plasmons cannot explain the Lorentzian type photoconductivity.

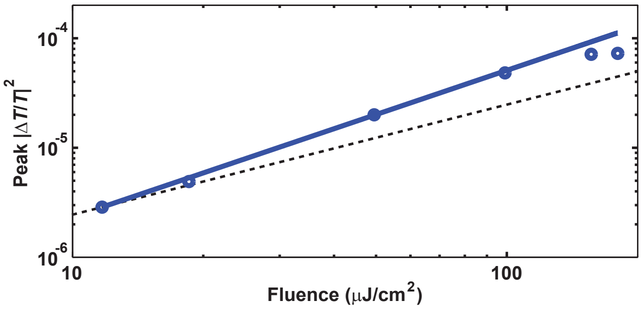

Supplementary Figure S3. Fluence dependence of the maximum pump induced transmission intensity change, measured in air. The broken line represents linear behaviour. From this it is clear that the data are super-linear, suggesting stimulated emission of terahertz photons. The solid line shows a least squares fit to the data, $|\Delta T/T|^2 \propto (\text{fluence})^{1.34}$.

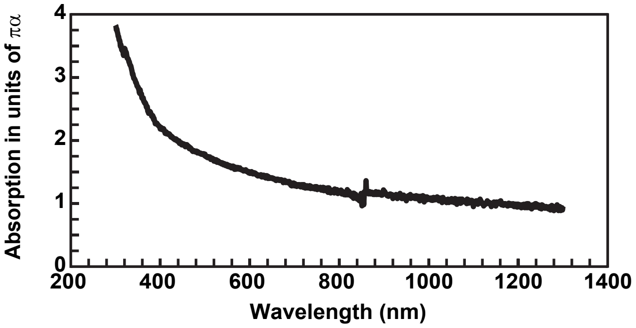

Supplementary Figure S4. UV-vis absorption spectra of sample. The near constant absorption of $\pi\alpha$ at optical wavelengths suggests monolayer growth[22]. The deviation from $\pi\alpha$ beyond 500 nm occurs because of nonlinear effects in the band structure of graphene far away from the Dirac point. The feature at 860 nm is an artefact of the spectrometer.

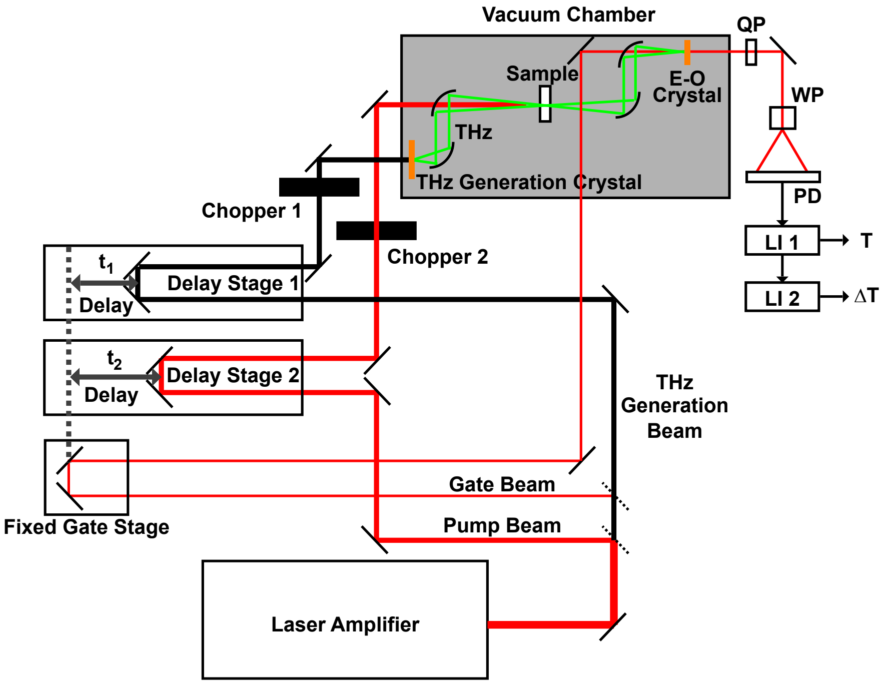

Supplementary Figure S5. Schematic diagram of the apparatus used for terahertz spectroscopy experiments. The 800 nm output from a Ti:Sapphire regenerative amplifier is used to photoexcite the sample, to generate terahertz radiation, and to detect the terahertz electric field by electro-optic sampling. The path length of the pump and terahertz generation beams can be altered relative to the fixed gate beam, thus varying the time of arrival of the terahertz and pump pulses at the sample, t_1 and t_2 respectively, relative to the gate pulse.

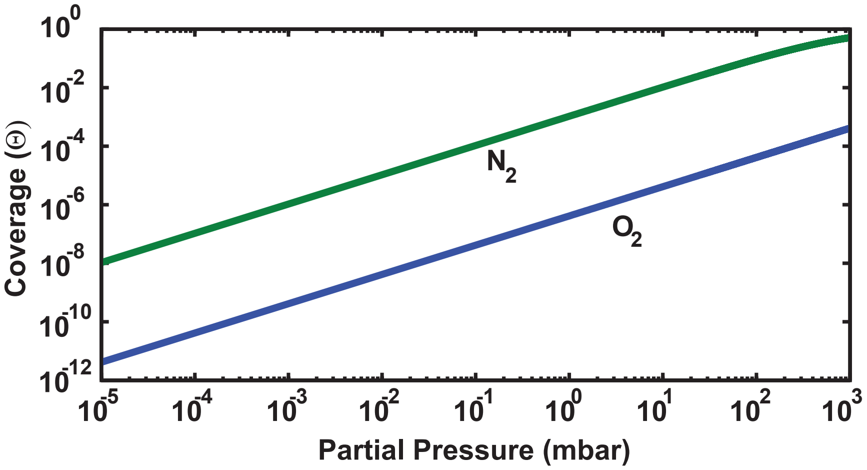

Supplementary Figure S6. Surface coverage of graphene with atmospheric gases. Calculated as a function of pressure using Langmuir theory. Temperature T was set to 300 K, and the other parameters were taken from Ref. 46 and are summarised in Supplementary Table S1.

Supplementary Tables

Species	E_B (kJ mol^{-1})	σ	ν (s^{-1})	m (g mol^{-1})
O_2	12	1	8×10^{13}	32
N_2	13	1	5×10^{10}	28
H_2O	46	1	9×10^{14}	18

Supplementary Table S1. Parameters used for Langmuir isotherm calculations. Taken from Ref. 46.

Supplementary Discussion

Terahertz Transmission

In the terahertz (THz) regime, the absorption of a graphene sheet is expected to be higher than at visible wavelengths, and to take a Drude free carrier form rather than a constant absorption[40]. To investigate this for our samples, we used terahertz time domain spectroscopy without photoexciting the sample. The transmission of the graphene, T, can be found from the transmission through the graphene and its quartz substrate, T_{sample}, and the transmission through the quartz substrate alone, T_{quartz}. Fourier transforming these time domain measurements yields $T(\omega) = T_{\mathrm{sample}}(\omega)/T_{\mathrm{quartz}}(\omega)$.

We recorded the non-photoexcited transmission of the sample in all four atmosphere types used in the photoconductivity measurements: vacuum, N_2, ambient air and O_2. These data are presented in Supplementary Figure S1a-d. From these data, the real part of the complex conductivity of graphene can be extracted using[41]

$$\sigma(\omega) = \frac{1 + n_{\mathrm{s}}}{Z_0} \left(\frac{1}{|T(\omega)|} - 1 \right), \tag{S1}$$

where Z_0 is the impedance of free space, $Z_0 = 377\,\Omega$, and n_{s} is the refractive index of the quartz substrate (Supplementary Figure S1e-f). Due to small mismatches in thickness between the graphene on quartz sample and quartz reference, the imaginary part of the conductivity cannot be reliably calculated for these samples. However, previous studies have shown $Im(\sigma)$ to be negligible for graphene in the terahertz region[41,42].

Both transmission and conductivity in all environments are roughly uniform and featureless over 3 THz, suggesting that the Drude scattering rate is higher than the bandwidth of our measurements[41]. It should be noted that the sensitivity of these measurements is lower than the pump-probe measurements of the main paper due to difference between the sample and reference substrate. There is no evidence of a bandgap opening due to adsorption of gas molecules, as we suggest in the main paper could cause the observed photoconductivity. However, in heavily p-doped graphene, such a bandgap would not be expected to be observable in terahertz transmission measurements as there are no occupied electron states near the top of the valance band available to be excited by low energy terahertz photons.

Fluence dependence of photoconductivity

Using optically excited terahertz spectroscopy, we observed a Lorentzian type photoconductivity, in contrast to the Drude photoconductivity measured by previous authors. One explanation of a Lorentzian photoconductivity in other materials is the photoexcitation of plasmons[44]. In order to investigate the possibility of a plasmon induced photoconductivity, we repeated the measurements at one tenth of the pump beam fluence, $18\,\mu\mathrm{J/cm}^2$ as opposed to $180\,\mu\mathrm{J/cm}^2$ used previously.

In plasmonic systems, the Lorentzian peak frequency, ω_0, is dependent upon carrier density, n. In graphene, $\omega_0 \propto n^{1/4}$, due to the nature of the two-dimensional Dirac carriers[37]. As the photoexcited carrier density is related to the pump fluence, a reduction in pump fluence would be expected to lower the frequency of the plasmon resonance.

Supplementary Figure S2 shows a comparison of the photoconductivity of graphene in air at 2 ps after photoexcitation by the high and low fluence pump. The lower fluence pump yields a smaller magnitude of photoconductivity, as it photoexcites fewer carriers. However, the Lorentzian peak frequency, ω_0, does not change with fluence, as would be expected for a plasmon dominated photoconductivity. Thus we conclude that the excitation of plasmons cannot explain our observations.

We further investigated the pump fluence dependence of the negative photoinduced change in conductivity using time domain pump-probe data (such as displayed in Figure 3 of the main paper). Supplementary Figure S3 shows the $|\Delta T/T|^2$, which is proportional to the intensity change in transmitted terahertz photons, as a function of the visible (800nm) photon fluence incident on a graphene sample in air.

The dashed line illustrates a linear relation while the solid line shows the result of a power law fit, $|\Delta T/T|^2 = A(\text{fluence})^\alpha$. Best agreement with data was obtained for $\alpha = 1.34$, in accordance with slightly superlinear behaviour. This behaviour may for example arise from an enhanced density of states available for stimulated downward transitions in the spectral range of the terahertz pulse with increasing visible pump fluence.

Supplementary Methods

Characterisation

For additional characterisation of the sample, the absorption spectrum of the graphene sheet was measured (using a Perkin-Elmer Lambda 9 UV-visible-NIR Spectrophotometer). Due to a constant optical conductivity near the Dirac point, where the conduction and valance bands meet, a graphene monolayer has a constant absorption of $\pi\alpha$, where α is the fine structure constant[22]. Each additional graphene layer adds an extra factor of $\pi\alpha$ to the absorption. Thus the optical absorption can be used to estimate the number of graphene layers.

In Supplementary Figure S4, we present the optical absorption spectrum of the graphene sample. The absorption in the far-IR to visible wavelength range is almost a constant $\pi\alpha$. Combined with the monolayer–like characteristics observed in the Raman and AFM measurements, this suggests the sample consists of mainly uniform monolayer graphene. The absorption increases beyond 500 nm because of the non-linearity of the band structure at energies far from the Dirac point.

Fitting Parameters

We fitted the photoconductivity in O_2, N_2 and air with a Lorentzian model of the form

$$\sigma_{\text{Lorentz}} \propto \frac{i\omega}{\omega^2 - \omega_0^2 + i\omega\Gamma}. \tag{S2}$$

As ω_0 is determined by the frequency at which the measured $\text{Im}(\Delta\sigma) = 0$, the only free parameter was the scattering rate, Γ. The fit yielded a value of $\Gamma = 10\,\text{THz}$ for all three gaseous atmospheres, with standard errors of 0.8, 2.6 and 1.5 THz for O_2, N_2 and air respectively.

Terahertz Spectroscopy Experimental Set-Up

The experimental arrangement used for terahertz time domain spectroscopy is displayed in Supplementary Figure S5. The output of a Ti:Sapphire laser amplifier is split into three beams: a pump beam to photoexcite the sample; a terahertz generation beam to produce terahertz radiation by optical rectification in a 2 mm GaP crystal; and a gate beam to detect the electric field of the terahertz pulse by electro-optic sampling[45]. Using a quarter waveplate (QP) and a Wollaston prism (WP), the gate beam is separated into two spatially resolved polarisation components for detection by photo-diodes (PD), from which the pump induced change in the terahertz signal can be extracted by two lock-in amplifiers, LI1 and LI2, referenced to optical choppers 1 and 2 respectively. The correct phase of the lock-in amplifiers for each experiment is determined by observing the signal from a reference sample with a well known photoresponse (semi-insulating GaAs).

Variable delay stages in the terahertz generation and pump beams allow additional path length to be added to these beams, whereas the gate beam is held fixed. Adding additional path length to the terahertz generation beam alters the time between the arrival of the terahertz pulse and the 45 fs gate pulse at the electro-optic (E-O) crystal, t_1. By varying this time, the full dynamics of the terahertz pulse can be mapped. Alternatively, the time between the pump pulse and the gate pulse, t_2, can be varied. In order to measure the full pump-induced transmission change, as in Figure 2c of the main paper, the pump delay time t_2 is set to a fixed value before the terahertz pulse is measured by varying t_1. Thus the delay between the pump pulse and the sampled part of the terahertz pulse is constant. Such data can then be Fourier transformed to yield spectral information[45]. For pump–probe measurements, as in Figure 3 of the main paper, t_1 is held fixed so that only the peak of the terahertz field is detected, whilst varying t_2 to reveal an average of the terahertz response after photoexcitation.

Adsorption of Environmental Gases on Graphene

Simple Langmuir adsorption theory may be used to estimate the coverage of the surface of graphene with gas molecules. In Langmuir theory the fractional coverage of a surface with adsorbed gas molecules is

$$\Theta(p, T) = \frac{bp}{1 + bp}, \tag{S3}$$

where

$$b = \frac{\sigma}{\nu N_0 \sqrt{2\pi m k_B T}} \exp\left(\frac{E_B}{k_B T}\right). \tag{S4}$$

Here, E_B is the adsorption enthalpy, σ is the steric factor, ν is the Arrhenius factor for desorption, N_0 is the adsorption site density and m is the mass of the adsorbant[47].

The parameters used in the calculation are taken from literature values for graphite and are listed in Supplementary Table S1. For room air at a pressure of 10^{-5} mbar the calculated coverage of graphene with adsorbed gases is negligible: $\Theta_{\mathrm{N_2}} = 8 \times 10^{-9}$, $\Theta_{\mathrm{O_2}} = 8 \times 10^{-13}$, $\Theta_{\mathrm{H_2O}} = 4 \times 10^{-9}$.

Supplementary Figure S6 shows the calculated fractional coverage Θ of the surface of graphene with N_2 and O_2 molecules over the pressure range used in the experiments. At 1 atmosphere pressure of N_2 and O_2 the coverages are calculated to be $\Theta_{\mathrm{N_2}} = 0.51$ and $\Theta_{\mathrm{O_2}} = 4 \times 10^{-4}$ respectively.

Supplementary References

[40] J M Dawlaty, S Shivaraman, J Strait, P George, M Chandrashekhar, F Rana, M G Spencer, D Veksler, and Y Q Chen. Measurement of the optical absorption spectra of epitaxial graphene from terahertz to visible. *Appl. Phys. Lett.*, **93,** 131905 (2008).

[41] J L Tomaino, A D Jameson, J W Kevek, M J Paul, A M v d Zande, R A Barton, P L McEuen, E D Minot, and Y Lee. Terahertz imaging and spectroscopy of large-area single-layer graphene. *Opt. Express*, **19,** 141–146 (2011).

[42] I Maeng, S Lim, S J Chae, Y H Lee, H Choi and J Son. Gate-Controlled Nonlinear Conductivity of Dirac Fermion in Graphene Field-Effect Transistors Measured by Terahertz Time-Domain Spectroscopy. *Nano Lett.*, **12,** 11258–11265 (2010).

[43] M van Exter, C Fattinger, and D Grischkowsky. Terahertz time-domain spectroscopy of water vapor. *Opt. Lett.*, **14,** 1128–1130 (1989).

[44] P Parkinson, H J Joyce, Q Gao, H H Tan, X Zhang, J Zou, C Jagadish, L M Herz, and M B Johnston. Carrier lifetime and mobility enhancement in nearly defect-free core–shell nanowires measured using time-resolved terahertz spectroscopy. *Nano Lett.*, **9,** 3349–3353 (2009).

[45] M C Beard, G M Turner, and C A Schmuttenmaer. Transient photoconductivity in GaAs as measured by time-resolved terahertz spectroscopy. *Phys. Rev. B*, **62,** 15764-15777 (2000).

[46] H Ulbricht, R Zacharia, N Cindir and T Hertel. Thermal desorption of gases and solvents from graphite and carbon nanotube surfaces. *Carbon*, **44,** 2931–2942 (2006).

[47] H Ulbricht, G Moos and T Hertel. Physisorption of molecular oxygen on single-wall carbon nanotube bundles and graphite. *Phys. Rev. B*, **66,** 075404 (2002).